Electronic Supplementary Material (ESI) for Journal of Materials Chemistry A.

In-situ TEM Investigation of Electron Beam Induced Ultrafast Chemical Lithiation for Charging

Guan-Min Huang,[a] Chun-Wei Huang,[b] Nagesh Kumar,[c, d] Chih-Yang Huang, [a] Tseung-Yuen Tseng[c] and Wen-Wei Wu[1, e, f]*

[a] Department of Materials Science and Engineering, National Chiao Tung University, Hsinchu, 30010, Taiwan.
[b] Material and Chemical Research Laboratories, Nanotechnology Research Center, Industrial Technology Research Institute, Hsinchu 310, Taiwan.
[c] Department of Electronics Engineering, National Chiao Tung University, Hsinchu, 30010, Taiwan
[d] Centre of Nanotechnology, I.I.T. Roorkee, Roorkee 247667, India.
[e] Center for the Intelligent Semiconductor Nano-system Technology Research, National Chiao Tung University, Hsinchu 300, Taiwan.
[f] Frontier Research Center on Fundamental and Applied Sciences of Matters, National Tsing Hua University, Hsinchu 300, Taiwan.

[*]Corresponding author. Tel.: +886 03 5712121 55395; E-mail address: wwwu@mail.nctu.edu.tw (W. W. Wu).

Table of Contents:

Movie S2: In situ TEM observation of $NiFe_2O_4$/CNTs during the chemical lithiation process (another sample).
Movie S3: In situ TEM visualization of $NiFe_2O_4$/CNTs during the electrochemical lithiation process.
Movie S4: In situ TEM observation of LiF clusters under e-beam irradiation.

Supplementary Information

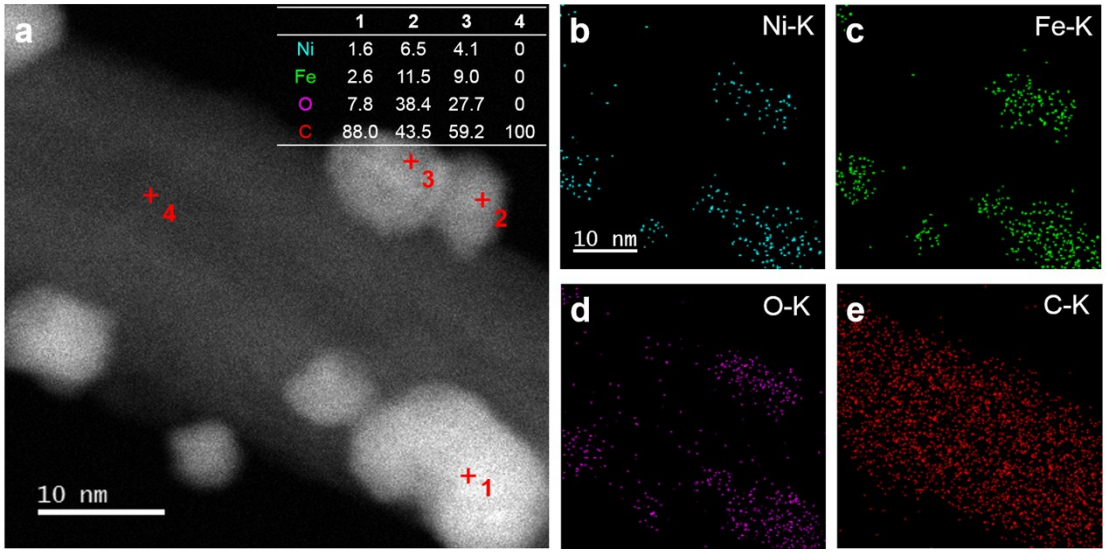

Figure S1. EDS analysis of the pristine electrode material $NiFe_2O_4$/CNTs. (a) STEM image of $NiFe_2O_4$ /CNTs showing CNTs decorated with $NiFe_2O_4$ nanoparticles and the table of chemical composition displayed in the inset. (b-e) Elemental distributions of Ni, Fe, O and C, respectively.

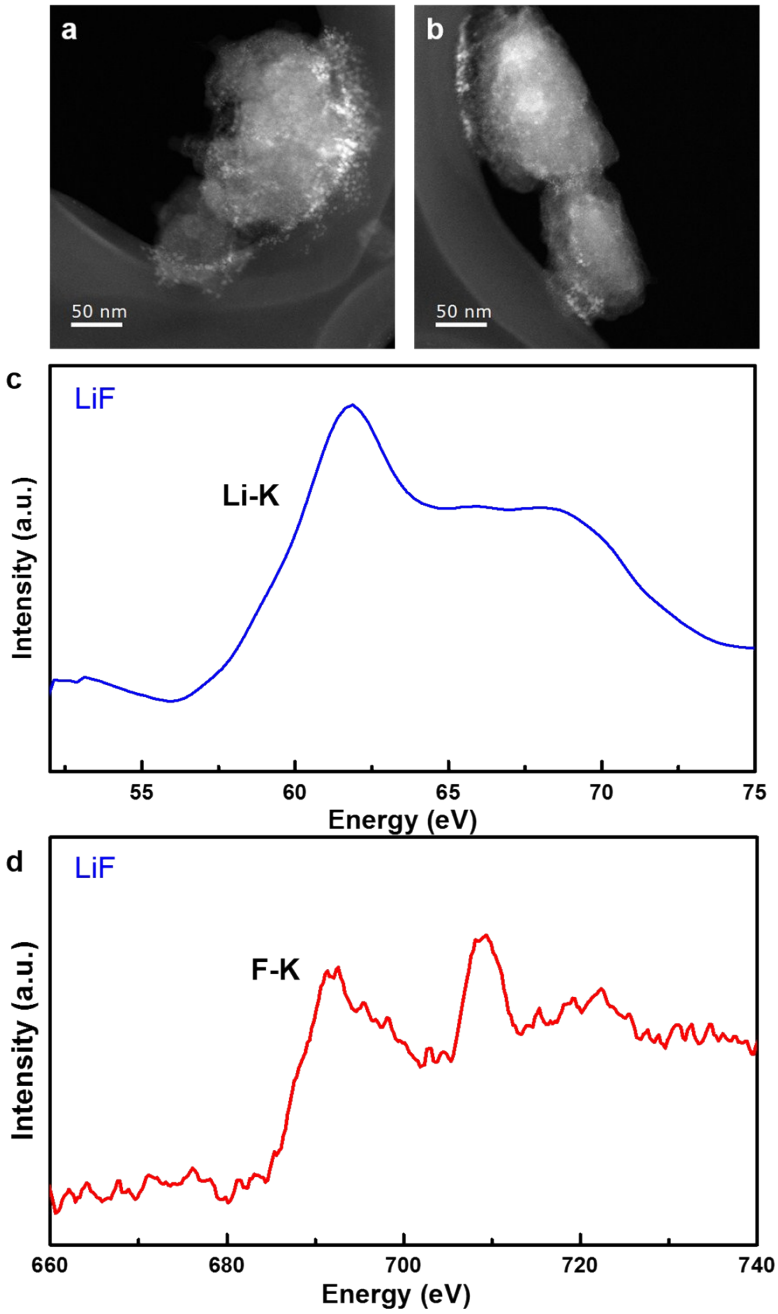

Figure S2. STEM images and EELS spectrum of LiF clusters. (a-b) The HAADF images of LiF clusters. (c) The peak of the Li-K edge and (d) F K-edge presented in spectrum corresponding to LiF.

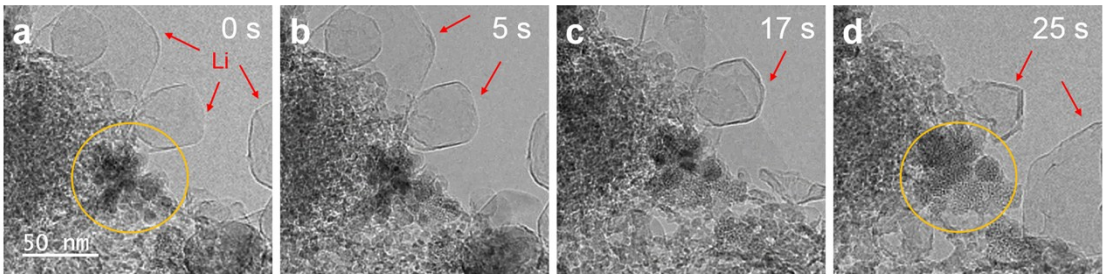

Figure S3. TEM images captured from the in situ video during chemical lithiation. (a-d) As e-beam irradiation acts on the materials, Li flakes are generated continuously and are followed by the lithiation of $NiFe_2O_4$. Red arrows and the yellow circle represent Li flakes and $NiFe_2O_4$, respectively.

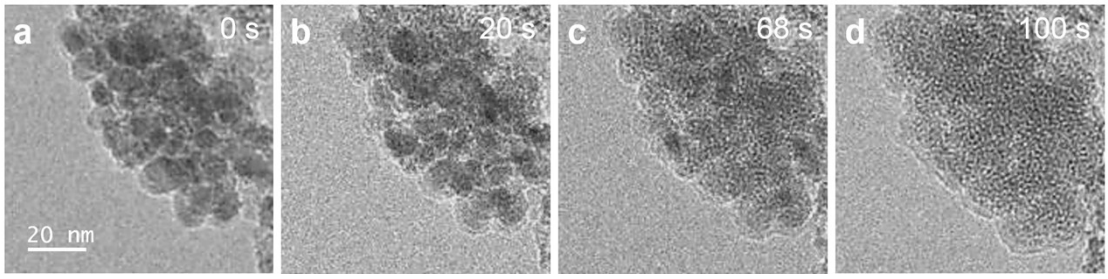

Figure S4. TEM images captured from the in situ video in the period of electrochemical lithiation. (a) Pristine $NiFe_2O_4$. (b-d) $NiFe_2O_4$ nanoparticles expand gradually and convert to the structure of Ni and Fe nanograins embedded in Li_2O matrix when a potential is applied.

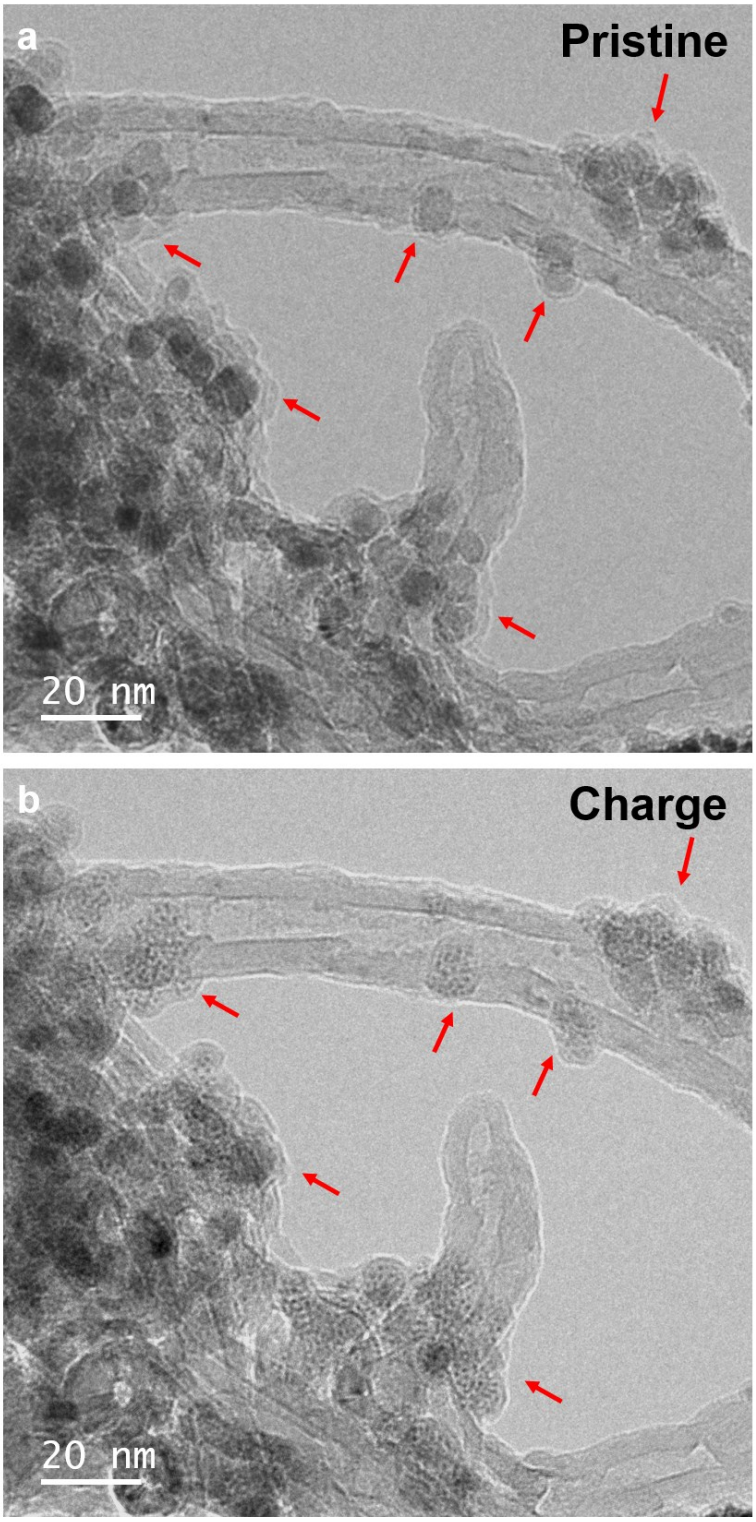

Figure S5. Structural variation in electrochemical lithiation under e-beam shielded. (a) Pristine $NiFe_2O_4$/CNTs. (b) $NiFe_2O_4$ nanoparticles transformed to Ni and Fe nanograins embedded in Li_2O matrix after charging (as red arrows labeled).

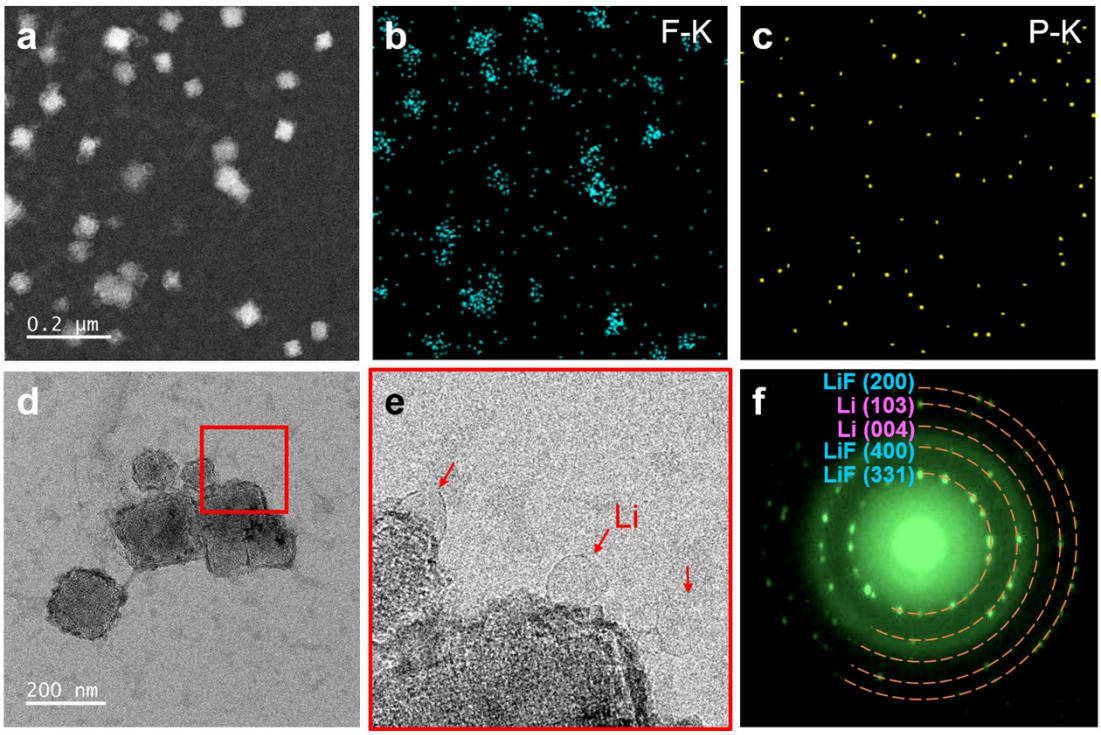

Figure S6. Morphology and elemental characterization of LiF clusters with e-beam irradiation. (a-c) STEM image and EDS mapping presenting elemental distribution of F and P. The morphology is demonstrated in (d) and (e). In panel (e), the magnified image of the area is marked by the red square, Li flakes had been generated (labeled by red arrows) on the surface of LiF clusters after e-beam irradiation, which coincided with the results of the SAED pattern in (f).

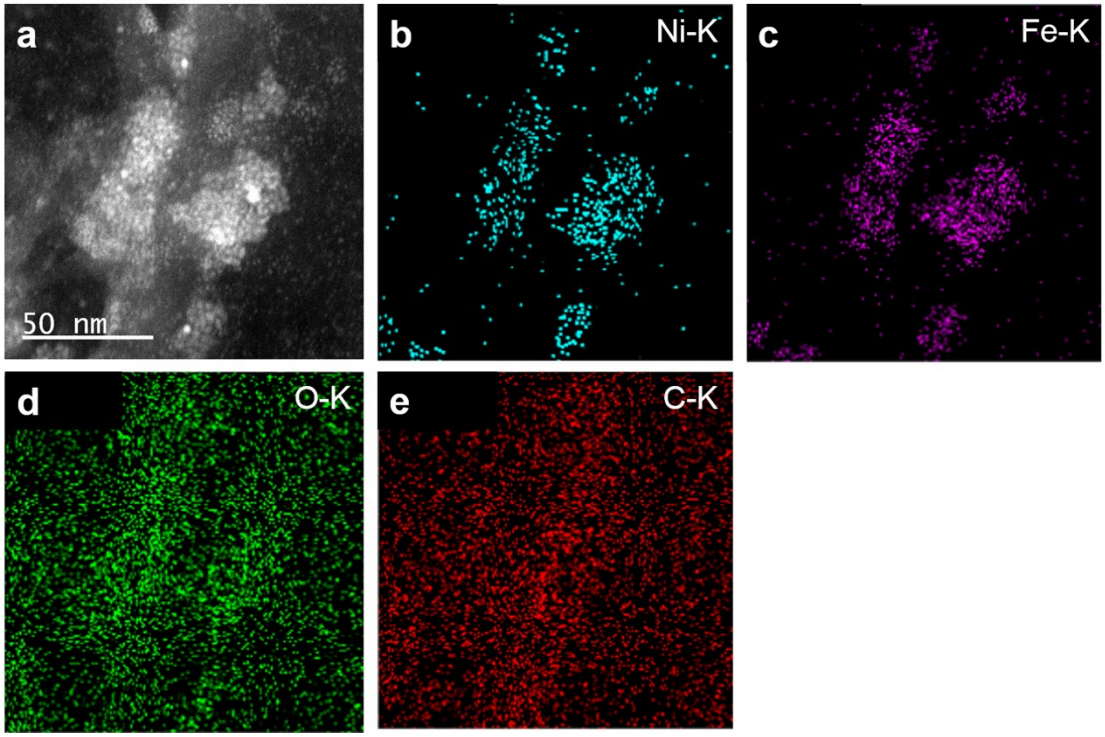

Figure S7. STEM images and EDS mapping of chemical lithiated $NiFe_2O_4$/CNTs. (a) STEM image of $NiFe_2O_4$/CNTs after chemical lithiation displays the numerous Ni and Fe nanograins dispersed in the Li_2O matrix. (b-e) Elemental distribution of Ni, Fe, O and C.

To provide the direct evidence and compare the mechanism of chemical lithiation with electrochemical lithiation, four in situ TEM movies are supplied as follows.

Supplementary movies

Movie S1: In situ TEM visualization of $NiFe_2O_4$/CNTs during the chemical lithiation process. When the e-beam acts on the composite material, the $NiFe_2O_4$ nanoparticles convert to 2-nm Ni and Fe nanograins embedded in the Li_2O matrix. The movie is played at original speed.

Movie S2: In situ TEM observation of $NiFe_2O_4$/CNTs during the chemical lithiation process (another sample). With the effect of e-beam irradiation, the formation of Li flakes and chemical lithiation is seen clearly in this video. The movie is played at 2x speed.

Movie S3: In situ TEM visualization of $NiFe_2O_4$/CNTs during the electrochemical lithiation process. When a potential of -5 V was applied against the cathode, it took a longer time to let the $NiFe_2O_4$ convert to 2-nm Ni and Fe nanograins embedded in the Li_2O matrix, which was same as the reaction of chemical lithiation. The movie is played at 8x speed.

Movie S4: In situ TEM observation of LiF clusters under e-beam irradiation. Several Li flakes were continuously generated from the LiF clusters. The movie is played at original speed.

Movie S5: In situ TEM Movie showing the continuous generation and shrinkage of Li flakes under e-beam irradiation for 60 s. Due to the low melting point (180.5 ℃) of Li, the Li flakes are easy to achieve "quasi-melting" condition, which leads to the shrinkage. The movie is played at original speed.